Th SRS2 14

Constrained Waveform Inversion - Automatic Salt Flooding with Inclusions

L. guasch* (Sub Salt Solutions Limited), M. Warner (Imperial College London) & F.J. Herrmann (University of British Columbia)

SUMMARY

The quality of the subsurface velocity model is most often the limiting factor in salt-affected seismic imaging. FWI can potentially improve the accuracy and resolution of such models, but realising this can be difficult in practice. Here we present constrained FWI results, using data from synthetic sub-salt models. We include constraints upon the set of allowable earth models; these include limitations upon the total variation norm of the velocity of the model, and upon the variation of velocity with depth such that negative velocity excursions are controlled. These constraints are progressively relaxed during iteration so that the final results are dominated by the data mismatch. The constraints act to steer the inversion towards geologically realistic models. We have applied this approach to a modified version of the SEAM salt model where we have introduced salt inclusions and a re-entrant structure at top salt. We are able to recover an accurate model of the dirty salt body starting from a one-dimensional velocity model.

Introduction

Established workflows for sub-salt seismic imaging and velocity-model building typically involve travel-time tomography to remove shallow residual moveout, picking of top salt on depth-migrated images, followed by salt flooding of the velocity model, remigration, picking of bottom salt, followed by sediment flooding and further tomography. Such workflows often involve multiple iterations, expert guidance, and manual scenario testing, and as a consequence can be both time-consuming and costly. When salt bodies contain inclusions of rafted sediment and other internal heterogeneities, these workflows can be particularly challenging. Full-waveform inversion has been used successfully to supplement this approach, but it does not normally serve to replace any part of this workflow.

In this paper, we show that suitably constrained full-waveform inversion can be used as the principal velocity-model building tool in complex salt-affected and sub-salt datasets. This approach can deal with both clean and dirty salt, and can begin from simple low-cost velocity models. Constrained waveform inversion does not require explicit picking of top and bottom salt; rather it acts in effect as a method of automated salt and sediment flooding, but in a fashion that has proper regard for heterogeneity within the salt. Following Esser et al. (2015), we use both the total-variation norm of the updated model, and asymmetric hinge-loss applied in a vertical direction, to constrain the recovered model, progressively relaxing these constraints as the inversion proceeds.

Method

Full-waveform inversion involves the minimisation of an objective function f of the form

$$f(\mathbf{m}) = \|\mathbf{p}(\mathbf{m}) - \mathbf{d}\|^2$$

where **m** is the model to be recovered, **p** is the data predicted using that model, and **d** is the observed data. For velocity models to be geologically plausible, they need to have certain additional characteristics. The basis of our approach is to modify this simple FWI equation so that it has regard for these characteristics, and in particular for the total variation of the updated model and for the asymmetric one-sided hinge-loss variation of the updated model in the vertical direction.

To do this, we define the total-variation norm of the model to be

$$\|\mathbf{m}\|_{\mathrm{TV}} = \sum \sqrt{\left(m_{i+1,j,k} - m_{i,j,k}\right)^2 + \left(m_{i,j+1,k} - m_{i,j,k}\right)^2 + \left(m_{i,j,k+1} - m_{i,j,k}\right)^2}$$

where $m_{i,j,k}$ is the value of the slowness squared at the mesh point $(i\ ,j\ ,k)$ which forms part of the regular mesh on which the model **m** is defined, and the sum is over all points in the interior of the model. Small values of this norm will represent models that have minimal variation in their velocity between adjacent points in the mesh, and its use as part of FWI will tend to lead to models that are piecewise smooth.

We further define the hinge-loss norm to be

$$\|\mathbf{m}\|_{\mathrm{HL}} = \sum \max\left(0, m_{i,j,k+1} - m_{i,j,k}\right)$$

where the function "max" selects the larger of its two arguments, and the k-axis is vertical with k increasing downwards. This norm has no regard to those portions of the model where velocity stays constant or where it increases with depth; small values of the norm will represent models that have minimal decrease in their velocity with depth.

Model norms of this form can be introduced by adding penalty terms into the objective function. Here however we adopt a different approach (Esser et al., 2010, 2015), and treat the characteristics that we wish to preserve and promote as constraints. That is we seek to minimise:

$$f(\mathbf{m}) = \|\mathbf{p}(\mathbf{m}) - \mathbf{d}\|^2 \quad \text{subject to} \quad \begin{array}{l} \|\mathbf{m}\|_{\mathrm{TV}} \le \delta \\ \|\mathbf{m}\|_{\mathrm{HL}} \le \varepsilon \\ \left\{\mathbf{m} : m_{i,j,k} \in m_{\min} \le m_{i,j,k} \le m_{\max}\right\} \end{array}$$

where δ and ε are constraints that exclude all models that have norms larger than these values, and the final box constraint excludes models that contain any values that lie outside a permitted interval defined by $m_{\min}$ and $m_{\max}$. Small values of δ will tend to supress all variation of velocity within the model, whereas small values of ε will allow increases of velocity with depth but will tend to supress any decrease of velocity with depth. The strategy that we adopt then is to start with a simple smooth velocity model, and with small values of ε and δ. When the inversion begins, strong reflections in the observed from the sea bottom and from top salt will tend to produce sudden increases in velocity at those positions, but the strong constraints will tend to supress all other velocity variations.

As the inversion proceeds, we progressively relax the constraints, increasing the values of δ and ε, so that the data can more strongly influence the recovered model. At some point, reflections from bottom salt, and from heterogeneities within the salt will be sufficient to overcome the constraints, and these structures will then begin to appear in the model. At the end of the inversion, the constraints will have been significantly reduced so that the final model is influenced almost entirely by the data and not the constraints. However, the constraints will have acted during the inversion to steer the inversion towards more geologically-plausible models, and so avoid falling into the countless implausible local minima that otherwise exist in the region between the starting and final models.

Results

We have applied this approach to synthetic acoustic data generated from a portion of the SEAM sub-salt model modified to add additional heterogeneity within a rugose salt body, Figure 1. We have included a sub-horizontal inclusion to represent rafted sediment, a sub-vertical inclusion to represent a salt-weld or similar feature, and a re-entrant structure surrounding a salient inclusion at top salt of the kind that can cause particular problems in workflows that require explicit identification of top salt.

Figure 2 shows two contrasting starting models together with the final models generated from these using conventional FWI. The synthetic acquisition assumes a fixed 8-km receiver spread near the top of the water column containing 200 receivers; 100 sources were fired into this spread located across the top of the model. The inversion ran in the time domain, starting at 3 Hz, and progressing by stages to a maximum frequency of 12 Hz.

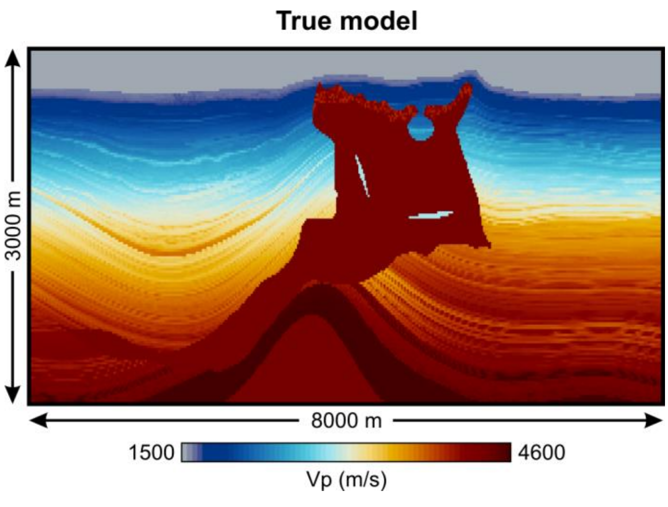

Figure 1 *The true velocity model used for this study. The model is based upon a part of the SEAM model (Fehle & Keliher, 2011) with the addition of two inclusions within the salt together with a re-entrant feature at top salt.*

Figure 2a shows a high-quality starting model obtained by smoothing a version of the starting model that does not contain the three inclusions. This quality of starting model is likely to be at or beyond the capability of the best conventional model-building workflows especially in the sub-salt portions of the model. Figure 2c shows the results of conventional FWI obtained using this starting model. The inversion has recovered all three inclusions, and has sharpened and improved the model everywhere. The resolution of the inclusions is limited principally only by the maximum frequency and limited acquisition aperture used in the inversion. This result demonstrates that conventional FWI can improve salt-affected velocity models when combined with an extremely good starting model.

In contrast, Figure 2b shows a simple, low-resolution, starting model of the type that could be generated rapidly using time-migrated gathers, or even from regional compaction trends. It contains no initial salt body; the seabed geometry is correct and the water velocity is correct, but the water-bottom reflectivity is not correct. This model generates data that is cycle skipped at 3 Hz with respect to the data from the true model. Figure 2d shows the results of applying conventional FWI to this problem using the simple starting model. Clearly FWI has failed to recover anything useful in the final model, and this result is not surprising given the inadequacy of the starting point.

Figure 3 shows results obtained using constrained FWI employing both TV and HL constraints as outlined above. The starting model used was the simple model from Figure 2b that failed entirely when combined with conventional FWI. Figure 3a shows the results of constrained FWI at an early stage. Here the constraints are strong and only the strongest features in the seismic data are able to overcome them. The constraints have actually wiped out most features that were present in the starting model; they have started to build a top-salt boundary, and the hinge-loss constraint forces the resultant high-velocity body below this to extend to the base of the model.

Figures 3b and 3c show the results of later iterations obtained as the constraints are successively relaxed. This relaxation initially serves to build the salt body smoothly to the base of the model, but as the seismic data becomes relatively more important in the inversion, deeper structure, sedimentary layering and the beginnings of the inclusions start to appear. In Figure 3d, the inversion is complete. The constraints here have largely disappeared, and the seismic data alone dominates the form of the final model. The recovered model is now a close match to the true model except at the edges of the acquisition where there is little or no seismic data available to influence the model and so the constraints still dominate. Although this inversion began from the simple model, quantitative comparison shows that it provides a better match to the true model everywhere except near the model edges than does conventional FWI begun from the high-quality starting model.

Conclusions

FWI, constrained by total variation and vertical asymmetric hinge-loss variation, appears able to recover accurate models of top salt, salt inclusions, bottom salt, and sub-salt velocity structure starting from a simple inexpensive velocity model. This approach does not require picking of salt boundaries, salt and sediment flooding, repeated scenario testing or the application of reflection tomography. We are addressing the challenge of applying this methodology directly to field data, and will present the first results of that effort at the meeting. We thank Sub Salt for permission to publish this work.

References

Fehler, M. and P. J. Keliher, 2011, SEAM Phase I: Final report — Challenges of subsalt imaging in Tertiary basins, with emphasis on deepwater Gulf of Mexico: SEG.

Esser et al., 2010, A general framework for a class of first-order primal-dual algorithms for convex optimization in imaging science: SIAM Journal on Imaging Sciences, **3**, 1015–1046.

Esser et al., 2015, Automatic salt delineation: Wavefield reconstruction inversion with convex constraints, 85th Annual International Meeting, SEG, Expanded Abstracts, 1337-1340.

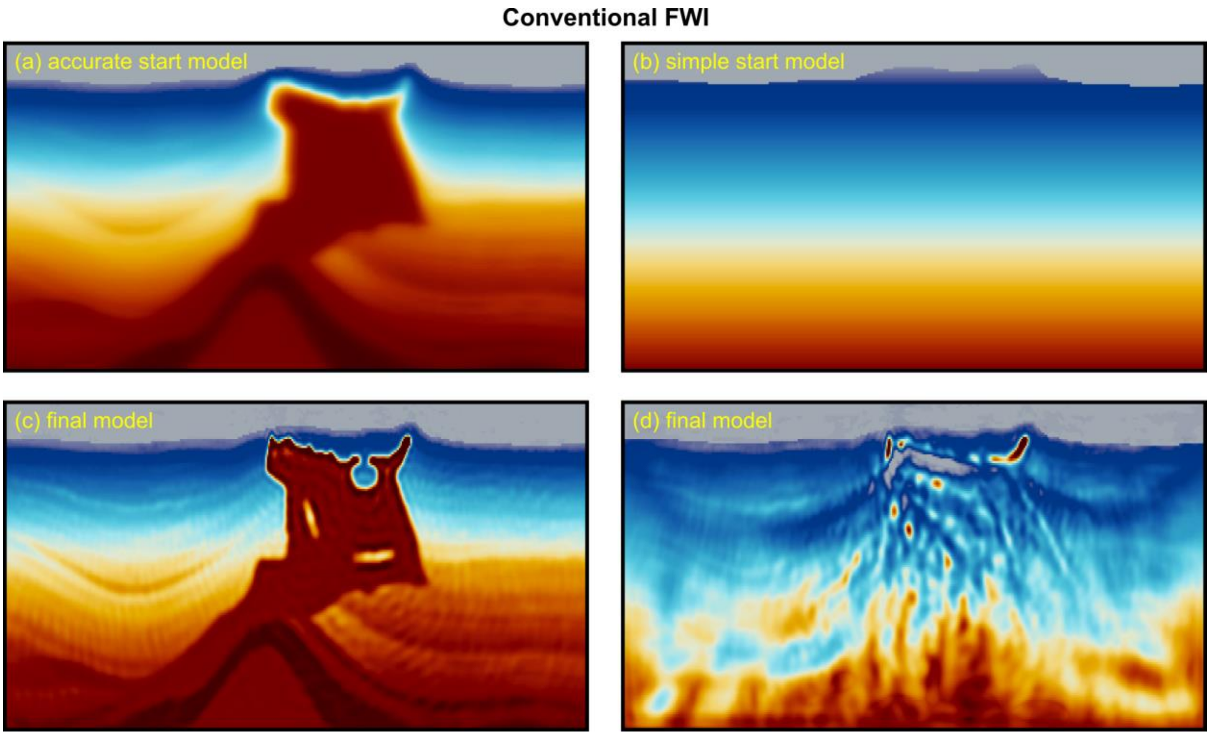

Figure 2 *Conventional FWI applied using two starting models. (a) A highly accurate starting model in which the salt body is already well defined. (b) A simple starting model that contains no initial salt body. (c) The model is well recovered by FWI when using the accurate start model. (d) The model is not recovered at all by conventional FWI when using the simple starting model.*

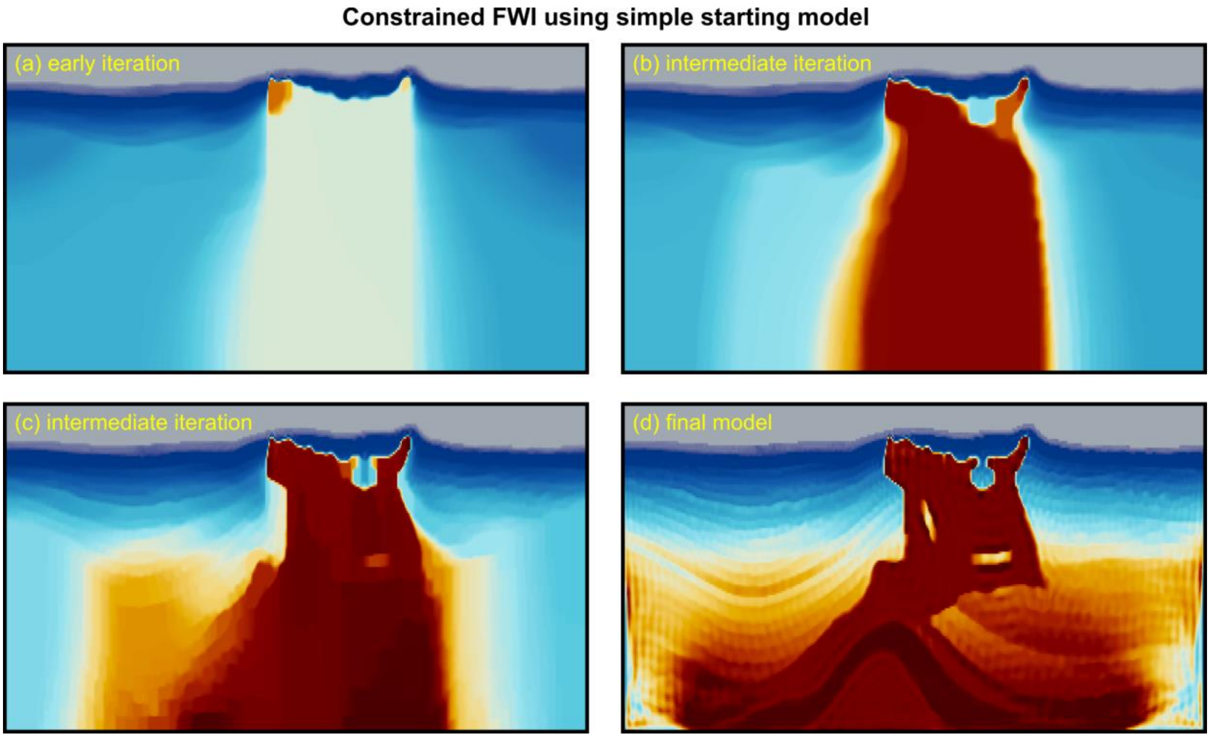

Figure 3 Constrained FWI applied using the simple starting model shown in Figure 2b. (a) The model obtained at an early stage when the constraints dominate. (b) & (c) Intermediate models obtained as the constraints are progressively relaxed. (d) The final model obtained when the constraints have been fully relaxed; there is a close match to the true model shown in Figure 1.